



# Paper microfluidic device for early diagnosis and prognosis of acute myocardial infarction via quantitative multiplex cardiac biomarker detection



Wei Yin Lim<sup>a</sup>, T. Malathi Thevarajah<sup>b</sup>, Boon Tong Goh<sup>c</sup>, Sook Mei Khor<sup>a,d,\*</sup>

<sup>a</sup> Department of Chemistry, Faculty of Science, University of Malaya, 50603 Kuala Lumpur, Malaysia

<sup>b</sup> Department of Pathology, Faculty of Medicine, University of Malaya, 50603 Kuala Lumpur, Malaysia

<sup>c</sup> Low Dimensional Materials Research Centre, Department of Physics, Faculty of Science, University of Malaya, 50603 Kuala Lumpur, Malaysia

<sup>d</sup> University Malaya Centre for Ionic Liquids (UMCIL), University of Malaya, 50603 Kuala Lumpur, Malaysia

## ARTICLE INFO

### Keywords:

Microfluidic paper-based device  
Troponin T  
Creatine kinase-MB  
Glycogen phosphorylase isoenzyme BB  
Acute myocardial infarction  
Multiplex detection

## ABSTRACT

The early detection of acute myocardial infarction (AMI) upon the onset of chest pain symptoms is crucial for patient survival. However, this detection is challenging, particularly without a persistent elevation of ST-segment reflected in an electrocardiogram or in blood tests. A majority of the available point-of-care testing devices allow accurate and rapid diagnosis of AMI. However, AMI diagnosis is reliable only at intermediate and later stages, with myocardial injury (> 6 h) and MI, based on the expression of specific cardiac biomarkers including troponin I or T (cTnI or cTnT), creatine kinase-MB (CK-MB), and myoglobin. Diagnosis at the early myocardial ischemia stage is not possible. To overcome this limitation, a sensitive and rapid microfluidic paper-based device ( $\mu$ PAD) was developed for the simultaneous detection of multiple cardiac biomarkers for the early and late diagnosis of AMI. The glycogen phosphorylase isoenzyme BB (GPBB) was detected during early (within first 4 h) ischemic myocardial injury. On the same  $\mu$ PAD platform, detection of prolonged elevation of levels of cTnT and CK-MB, which are only produced 6 h after the onset of chest pain in human serum, was possible. Sandwich immunoassay performed on the  $\mu$ PAD achieved reproducibility (RSD approximately 10% and intra- and inter-day precision (CV 10–20%, 99th percentile), as well as consistently stable test results for 28 days, with strong correlation ( $r^2 = 0.962$ ), using the standard Siemens Centaur XPT Immunoassay system. The present findings indicate the potential of the  $\mu$ PAD platform as a point-of-care device for the early diagnosis and prognosis of AMI.

## 1. Introduction

In the clinical setting, the term acute coronary syndrome (ACS) refers to a spectrum of clinical presentation for symptoms of ischemia (inadequate blood supply to heart), such as unstable angina, non-ST elevation myocardial infarction (STEMI), and STEMI (Overbaugh, 2009). Chest pain is one of the most common complaints among patients presenting to the emergency department. The diagnosis of ACS is dependent on evidence of myocardial ischemia on an electrocardiogram (ECG) and evidence of myocardial injury by determining the levels of cardiac biochemical markers (Ryu et al., 2011). For patients with chest pain, no evidence of myocardial injury based on the levels of cardiac biomarkers in the blood is considered to present unstable angina, whereas patients presenting with positive cardiac biomarkers, with or without electrocardiographic ST-segment depression or T wave

inversion, are undergoing non-STEMI due to a relatively small damage of heart muscles (Anderson et al., 2007; Bertrand et al., 2000). Furthermore, patients with ST-segment elevation on an ECG due to high damage extent of heart muscles indicate acute STEMI (Van de Werf et al., 2003) (Supplementary material Fig. S1).

In clinical trials, patients with chest pain and suspected ACS may be referred urgently to the emergency department and undergo ECG monitoring to aid in risk stratification (Lang et al., 2000). However, misinterpretation of findings on ECG accounts for 23–40% of misdiagnosed MI cases (Kontos et al., 2010). Due to ST-elevation, MI can be readily diagnosed with culprit ECG findings. However, for non-ST elevation, MI diagnoses are more challenging. Therefore, serial cardiac biomarker sampling is crucial for the diagnosis of acute MI in patients with non-diagnostic ECGs or chest discomfort symptom. Serial measurement of cardiac biomarkers of myocardial injury, such as cardiac

\* Corresponding author at: Department of Chemistry, Faculty of Science, University of Malaya, 50603 Kuala Lumpur, Malaysia.  
E-mail address: [naomikh@um.edu.my](mailto:naomikh@um.edu.my) (S.M. Khor).

<https://doi.org/10.1016/j.bios.2018.12.049>

Received 1 October 2018; Received in revised form 11 December 2018; Accepted 28 December 2018

Available online 09 January 2019

0956-5663/© 2019 Elsevier B.V. All rights reserved.

troponin (T or I), creatine kinase-MB (CK-MB), and myoglobin, are widely accepted as important determinants in ruling out MI in the emergency department (Al-Hadi and Fox, 2009; De Winter et al., 1995).

Currently available routine biomarkers of myocardial injury exhibit inadequate sensitivity for determining early MI, and none of these can be used to detect myocardial ischemia. Cardiac troponin (T or I) and CK-MB are only detectable for myocardial injury after 6 h of chest pain onset, and repeated measurement is necessary at 8–12 h after admission if a negative result is obtained at initial presentation (< 6 h) (Bertrand et al., 2000). Moreover, the earliest marker, myoglobin, which is detectable within the first 3 h of chest pain onset, is reportedly more specific for skeletal muscle injury than that for myocardial injury (De Winter et al., 1995; Mair et al., 1992). Hence, early diagnosis of acute chest pain by blood testing is still difficult in patients without persistent ST-segment elevation as most of these patients have been diagnosed as having unstable angina because of myocardial ischemia during initial presentation, with no elevation of cardiac marker levels (Mythili and Malathi, 2015). Early diagnosis of ischemic myocardial injury is essential for effective management of patients suspected with ACS, thereby avoiding life-threatening situations, such as heart attack (MI).

To overcome these limitations, glycogen phosphorylase isoenzyme BB (GPBB), which can diagnose myocardial injury and ischemia, was introduced as a reliable early marker to replace myoglobin for detection of myocardial injury (Bozkurt et al., 2011; Cubranic et al., 2012). GPBB activation in myocardial ischemia occurs because of an increase in glycogen degradation, which releases GPBB in the blood circulation within the first 4 h after chest pain onset before myoglobin, CK-MB, and troponins.

With the aim of miniaturizing the immunoassay procedures presently done at the central laboratory to a portable device that can be more widely used, and to reduce the waiting time for emergency room patients, lateral flow assays have been developed and are commercially available as point-of-care testing (POCT) devices from a variety of manufacturers for cardiac biomarker measurement in single and/or multiplex strategy for qualitative and/or quantitative detection with a portable reader (Amundson and Apple, 2015; McDonnell et al., 2009). All the troponin (T or I), CK-MB, and myoglobin analytes can be read qualitatively based on the color change and quantified individually and/or simultaneously with a reader within approximately 10–20 min after addition of the sample to the POCT device. Other methods studied more recently include fluorescence (Cai et al., 2018; Cho et al., 2014; Kim et al., 2014; Lee et al., 2013), magnetic beads (Ryu et al., 2011), and surface enhance Raman spectroscopy (SERS) tags (Zhang et al., 2018a) to enhance the detection sensitivity at lower concentrations and improve the wider dynamic range to cover the clinical symptoms. However, a dedicated reader is required for quantification of fluorescence or Raman signal (Table 1).

Moreover, lateral flow assays have some limitations in terms of flexibility in platform design for multianalyte detection and detection sensitivity for multi-analytes on a single test-strip. Owing to space limitation on a lateral flow strip, additional test lines are always drawn over a piece of membrane or few strips are overlapped together at the sides of the sample pad for multiplex analyte detection. This attempt does not increase the risk of false binding, since each assay is performed in parallel and independently, which removes the possibility of cross-contamination. The main drawback of this approach, however, is the amount of sample required, which increases as a function of the number of strips added (and consequently of biomarkers to be measured). Thus, it is difficult to construct a flexible design on a lateral flow test strip, such as including several reaction zones on the membrane. Additionally, the detection sensitivity for multiplex assay on a single test strip may be reduced because of the use of large amounts of capturing and labeled detecting antibodies, which may increase the risk of false positivity due to non-specific binding with non-target analytes. However, this limitation depends on whether the labeled antibodies are embedded in the lateral flow device and encounter all the capturing

antibodies during their flow. This problem has been not solved. Thus, the lateral flow assay limits the number and types of biomarkers that can be detected in a multiplex assay. Several research studies have been reported where smartphone-based test strip readers based on color analysis were used for various applications (Lopez-Ruiz et al., 2014; Oncescu et al., 2014, 2013; Shen et al., 2012). However, the commercial lateral flow assays that are currently available usually require a proper readout device for highly sensitive and quantitative detection during clinical diagnostic testing.

Herein, the microfluidic paper-based device ( $\mu$ PAD) was tested and demonstrated to exhibit high multiplexing capability and flexibility in the assay design. This design could be easily adapted to paper by various fabrication designs (Dincer et al., 2017). Moreover, the detection sensitivity of the multiplex assay on the fabricated  $\mu$ PAD could be further enhanced by utilizing numerous antibody conjugates for specific multiplex analyte detection. Nanoparticles (NPs) are preferably used as labels for colorimetric detection using  $\mu$ PAD. They offer distinct advantages. They allow multiplexed analysis by using differently colored NPs that are visible without an external excitation source (compared to fluorescence and quantum dot label) and are resistant to photobleaching. For instance, gold nanoparticles (AuNPs) (Choi et al., 2010; Quesada-Gonzalez and Merkoci, 2015; Rong-Hwa et al., 2010; Veigas et al., 2012) and silver nanoparticles (AgNPs) (Yen et al., 2015) can display different colors within the visible spectrum tuned by variations in shape and size that allow easy visual distinction. In addition, NPs also have high binding efficiencies with a relatively low usage of antibody during bioconjugation due to the larger surface area to volume ratio (Arruebo et al., 2009).

To overcome the requirement of an expensive analyzer and/or reader for quantification, a reflectance detector, such as a mobile phone camera and/or scanner, was presently explored as an alternative low-cost and portable readout device that could be used with the  $\mu$ PAD for colorimetric detection. The intensity of color generated in a spatially defined zone on  $\mu$ PAD is converted to a number of pixels based on the RGB (red/green/blue) color analysis to generate a calibration plot for any quantitative analyte measurement (Martinez et al., 2010; Sechi et al., 2013).

In the present study, we aimed to develop a  $\mu$ PAD for multiple marker detection for diagnosis of AMI using early (GPBB) and late (CK-MB and cTnT) cardiac biomarkers (Supplementary material Fig. S2). Considering the fact that none of the single markers has exhibited sufficient diagnosis accuracy for acute myocardial infarction, a novel combination of these three specific cardiac biomarkers, viz., GPBB for early diagnosis (within the first 4 h) and cTnT and CK-MB for late after symptom onset (> 6 h) and prognosis of AMI (7–14 days), was incorporated into one device (Scheme 1). This enables the identification of multiplex biomarker release profiles for improved sensitivity and can identify MI (STEMI) and at-risk patients (non-STEMI and unstable angina) with a possible life-threatening cardiac event. The  $\mu$ PAD was fabricated by a simple and rapid fabrication technique (approximately 5 min) involving wax printing on a paper substrate in the form of a nitrocellulose (NC) membrane card using a solid wax printer (Fuji Xerox ColorQube 8870) to permit multiplexing branched flow into separate test zone(s) by capillary action for simultaneous multiplex detection (Supplementary material Fig. S3). The protocol was slightly modified from that of Carrilho et al. (2009a). To enhance the specificity, sensitivity, and visual judgment of the multiplexing assay, the nanomaterial used as optical labels (AuNPs, AgNPs, and gold urchin NPs) were separately conjugated with their specific detecting antibody to provide a distinct visible color as the colorimetric signal, e.g., AuNPs–cTnT, red; AgNPs–GPBB, yellow; and gold urchin NPs–CK-MB, purple. The color labels were assessed using a camera (with imaging software) to quantitatively measure the color intensity produced at the test zone(s). This is because the light reflected from each surface of the test zone(s) can be detected easily with the available reflectance detectors, such as a desktop scanner, digital camera, or phone camera.

**Table 1**  
Comparison of cardiac point-of-care (POC) devices for (a) quantitative and (b) qualitative analysis used in diagnosis of acute myocardial infarction.

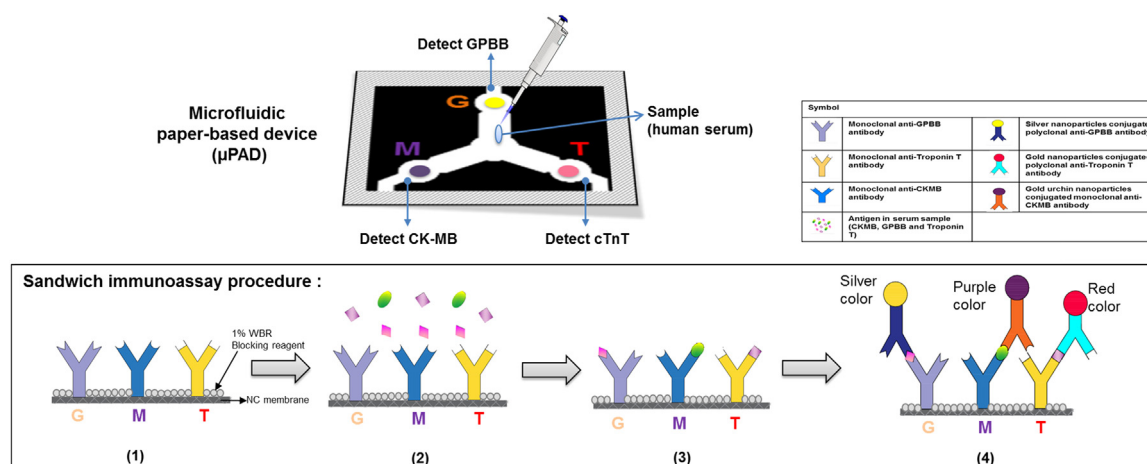
Name	Type of assay	Biomarker	Type of label	Volume of sample (µL)	Detection time (Min)	Limit of detection	Dynamic range (ng mL <sup>-1</sup> )	Advantages	Disadvantages
<b>(a)</b>									
<b>Quantitative</b>									
Under research	S	● cTnI	Red fluorescent dye (Nile-red) with microsphere produced by styrene and acrylic acid	75	< 15	● 0.016 ng mL <sup>-1</sup>	● 0–40	<ul style="list-style-type: none"> <li>● Highly sensitive and increases the wide dynamic range</li> <li>● Reduces background noise interference signal by red fluorescence inside the microsphere</li> <li>● Magnetic labels allow for the detection of the signal from inside the membrane, whereas other optical labels are visible only within 10 µm from the surface of the membrane</li> <li>● Increases the detection sensitivity by oriented immobilization of antibodies on magnetic beads</li> <li>● Simultaneously measures three cardiac biomarkers to diagnose acute myocardial infarction</li> <li>● Introduces simple cross-flow washing after antigen–antibody binding to resolve the chronic background problem</li> <li>● Simultaneously measures three cardiac biomarkers to diagnose acute myocardial infarction</li> <li>● More stable than fluorescent imaging</li> <li>● High enhancement factor because of plasmonic nanostructures of SERS tag</li> <li>● Improves limit of detection to pg mL<sup>-1</sup> (decreased by three orders of magnitude)</li> <li>● Reduces turnaround time</li> <li>● Can be qualitatively detected by the naked eye</li> <li>● Increases the detection sensitivity in lower biomarker levels</li> </ul>	<ul style="list-style-type: none"> <li>● Requires a fluorescent spectrophotometer for quantification</li> <li>● Requires UV-light for visual observation of the resulting signal</li> <li>● Requires giant magneto resistive (GMR) sensors for signal quantification</li> </ul>
	S	● cTnI	Magnetic beads	50	NA	● 0.01 ng mL <sup>-1</sup>	NA	<ul style="list-style-type: none"> <li>● Expands the reader system to up to three test modules (multi-port reader) connected with a control module for simultaneous multiplex analysis</li> </ul>	<ul style="list-style-type: none"> <li>● Limited quantitative dynamic range and limit of detection</li> </ul>
	M	(i) cTnI (ii) CK-MB (iii) Myoglobin	Alexa Fluor 647 fluorescent dye	80	15	(i) 0.05 ng mL <sup>-1</sup> (ii) NA (iii) NA	(i) 0.05–25 (ii) 0.2–100 (iii) 2.0–1000	<ul style="list-style-type: none"> <li>● Requires dedicated readers for quantification</li> </ul>	
	M	cTnI CK-MB Myoglobin	Core-shell SERS tags	100	7	0.44 pg mL <sup>-1</sup> 0.55 pg mL <sup>-1</sup> 3.2 pg mL <sup>-1</sup>	0.01–50 0.02–90 0.01–500	<ul style="list-style-type: none"> <li>● Requires Raman spectroscopy to measure the SERS signal quantitatively</li> </ul>	
Commercial	S	● cTnT	Gold nanoparticles	150	8–12	● 0.05 ng mL <sup>-1</sup>	● 0.1–2	<ul style="list-style-type: none"> <li>● Requires readout for quantification</li> </ul>	
	S	cTnI CK-MB Myoglobin	Fluorescent	250	15	0.19 ng mL <sup>-1</sup> 0.75 ng mL <sup>-1</sup> 2.7 ng mL <sup>-1</sup>	NA	<ul style="list-style-type: none"> <li>● For single use only (per cartridge)</li> <li>● More test cartridge required for serial testing of biomarkers</li> <li>● Requires customized readers for measuring the fluorescence intensity of the signal line</li> </ul>	
	S/M	cTnI CK-MB Myoglobin	Fluorescent latex	6 drops	15	0.03 ng mL <sup>-1</sup> 0.32 ng mL <sup>-1</sup> 2.4 ng mL <sup>-1</sup>	0–32 0–80 0–400		
This study	M	cTnT CK-MB	Microfluidic paper-based device	10	10	0.05 ng mL <sup>-1</sup>	0–200 0–100		

(continued on next page)

Table 1 (continued)

Name	Type of assay	Biomarker	Type of label	Volume of sample (µL)	Detection time (Min)	Limit of detection (ng mL <sup>-1</sup> )	Dynamic range (ng mL <sup>-1</sup> )	Advantages	Disadvantages	
(b) Commercial	*M	GPBB cTnI CK-MB Myoglobin	Nano-particles (gold, silver, and gold urchin)	6 drops	15	0.5 ng mL <sup>-1</sup>	0–100	the first 4 h and can distinguish between non-ST elevation myocardial infarction and unstable angina in early diagnosis and prognosis (> 6 h) of acute myocardial infarction		
						0.5 ng mL <sup>-1</sup>				<ul style="list-style-type: none"> <li>Colorimetric detection for qualitative, semi-quantitative, and quantitative analysis by using available phone camera and/or scanner</li> </ul>
						NA				
Lifesign MI TnI	*M	(i) cTnI (ii) CK-MB (iii) Myoglobin	Gold nanoparticles	120 (3 drops)	15	(i) 0.5 ng mL <sup>-1</sup> (ii) 5 ng mL <sup>-1</sup> (iii) 80 ng mL <sup>-1</sup>	NA		<ul style="list-style-type: none"> <li>Myoglobin is a non-cardiac specific marker and sensitive to skeletal injury</li> <li>Troponin and CK-MB markers are only detectable after 6 h of chest pain onset</li> </ul>	
						(i) 1.5 ng mL <sup>-1</sup> (ii) 5 ng mL <sup>-1</sup> (iii) 50 ng mL <sup>-1</sup>				
						NA				
Cortez AMI 3 IN 1 Test	*M	(i) cTnI (ii) CK-MB (iii) Myoglobin	Gold nanoparticles	80	15	0.5 ng mL <sup>-1</sup> 5 ng mL <sup>-1</sup> (i) 80 ng mL <sup>-1</sup>	NA			
Roche Trop T <sup>®</sup> Sensitive Rapid Assay	S	cTnT	Gold nanoparticles	150	15	0.1 ng mL <sup>-1</sup>	NA	<ul style="list-style-type: none"> <li>Standard biomarker for myocardial infarction diagnosis owing to its high sensitivity and specificity</li> <li>Useful for prognosis of myocardial infarction (7–14 days)</li> </ul>	<ul style="list-style-type: none"> <li>Not suitable for use as an early marker of myocardial necrosis (at the first 4 h after chest pain onset) and is only detectable after 4–6 h and peaks at 12–24 h</li> </ul>	

S, for single assay only; M, for multiplex assay performed individually on different strips/cartridges. NA- not available.



**Scheme 1.** Scheme of fabrication of the microfluidic paper-based device ( $\mu$ PAD) for multiplex detection of cardiac markers. It is designed with three reaction zones marked as G for GPBB, M for CK-MB, and T for troponin T and one sample zone at the center for multiplex detection. Sandwich immunoassay procedure: (1) Capture antibody was immobilized on the NC membrane at reaction zones G, M, and T. (2) Sample (10  $\mu$ L) was added to the central sample zone. (3) Target analyte specifically bound to the respective capturing antibody. (4) The target analyte was sandwiched between a capturing antibody and detecting antibody. Color signals were then observed from the labeled nanoparticles conjugate-detecting antibodies (yellow for GPBB, purple for CK-MB, and red for cTnT). (For interpretation of the references to color in this figure legend, the reader is referred to the web version of this article.)

Thus, the NPs utilized by the  $\mu$ PAD as labels are robust and simple, and allow qualitative, semi-quantitative, and quantitative determination of the biomarkers.

## 2. Materials and methods

Please refer to [Supplementary material](#) for Research Methodology.

## 3. Results and discussion

### 3.1. Qualitative detection of multiplex cardiac biomarkers on the fabricated $\mu$ PAD

Qualitative analysis in healthcare has become increasingly important to provide immediate results for the direct detection of the presence or absence of biomarkers in the sample to diagnose patients suspected of AMI. Qualitative test results can aid clinicians in decision-making at a critical moment for admitting a patient with MI. The incorporation of metal nanoparticles, viz., gold, silver, and gold urchin, as labels allows visual examination of the color signal at the reaction zone (s), resulting in qualitative (Yes/No) or semi-quantitative analysis. For qualitative assay, the color dot displayed at any reaction zone(s), G (GPBB), M (CK-MB), and T (cTnT), on the fabricated  $\mu$ PAD indicates the presence of the particular cardiac marker (positive result), whereas its absence indicates a negative result (Fig. 1). The intensity of the color dot in the test zones G, T, and M varies depending on the concentration of GPBB, cTnT, and CK-MB, respectively, present in the given sample. Hence, any shade of color displayed in test zone(s) should be considered as positive. For the fabricated  $\mu$ PAD, the cut-off levels for each cardiac biomarker were determined as 10  $\text{ng mL}^{-1}$  for GPBB, 5  $\text{ng mL}^{-1}$  for CK-MB, and 0.1  $\text{ng mL}^{-1}$  for cTnT (Supplementary material Table S1). The exact amounts of biomarkers (GPBB, CK-MB, and cTnT) used to generate colors as shown in Fig. 1 were 10  $\text{ng mL}^{-1}$ . Moreover, the qualitative test requires no measurement instruments and the user can observe colorimetric result easily by the naked eye based on the distinct color on the  $\mu$ PAD. To avoid wrong interpretation of a false-positive result due to the color stain of NPs conjugates at the reaction zone(s) of the  $\mu$ PAD, the colorimetric signal should be determined visually from approximately 30 mm from the color dot (1  $\mu$ L of volume) to 50 mm of the diameter of the reaction zone(s).

### 3.2. Semi-quantitative analysis of multiplex cardiac biomarkers on the fabricated $\mu$ PAD

Table 2 presents the reference chart based on the levels of multiple cardiac biomarkers, viz., (a) GPBB, (b) CK-MB, and (c) cTnT on the fabricated  $\mu$ PAD. The levels of the biomarkers were categorized into three risk categories. Higher levels were associated with increased damage (high risk), lower levels with less damage (moderate), and levels in a patient suspected with unstable angina (less risk), based on the 99th percentile upper reference limit in which the 99th percentile of a normal, healthy reference population as the decision level for the diagnosis of MI (Supplementary material Table S2). The semi-quantitative results on each reaction zone exhibit significantly different color intensity that is directly proportional to the concentration of the cardiac marker. The signal intensity on the fabricated  $\mu$ PADs slowly concentrated with the increase in the levels of the respective cardiac biomarkers (from left to right) and the degree of visibility of the color dot in each test zone (Table 2). Thus, darker intensity of the color dot on the fabricated  $\mu$ PAD is an indication of serious heart injury. The normal level of GPBB is 7  $\text{ng mL}^{-1}$  and peaks at 50  $\text{ng mL}^{-1}$  after AMI (Kaski and Holt, 2013). For CK-MB, the concentration is 1  $\text{ng mL}^{-1}$  and increases to 5–20-times on occurrence of AMI (Gupta et al., 2008; Qureshi et al., 2012). Elevated troponin T level, which is 3–4-times higher than the normal level 0.1  $\text{ng mL}^{-1}$ , is associated with a high mortality rate following MI (Ohman et al., 1996).

Based on semi-quantitative detection, the distinct color displayed on the fabricated  $\mu$ PAD can also be used to predict the extent of heart muscle damage. For instance, the presence of yellow color for GPBB only in the reaction zone G indicates patients suspected with ischemic myocardial injury in the early stage. The presence of purple color for CK-MB at the reaction zone M and red color for cTnT at the reaction zone T on the fabricated  $\mu$ PAD (absence of ischemia-specific marker, GPBB) indicates a patient suspected with myocardial injury and can prompt hospitalization for immediate treatment to avoid occurrence of infarction (heart attack). However, no semi-quantitative detection assays are available in the current clinical setting as cardiac biomarker measurements typically requires laboratory quantitative analysis in a hospital to obtain accurate results before patient admission.

The present semi-quantitative analysis is useful to assist physicians in decision-making for admission of ACS patients with moderate and high risk of myocardial injury, and to provide them with immediate and life-saving treatment without waiting for time-consuming laboratory

Expected qualitative result on fabricated $\mu$ PADs	Cardiac Markers			Qualitative test results on fabricated $\mu$ PADs	
	GPBB	CK-MB	cTnT	Phone Camera	Scanner
	-	-	-		
	+	-	-		
	-	-	+		
	-	+	-		
	+	+	+		

**Fig. 1.** Qualitative test results for cardiac marker detection on the fabricated  $\mu$ PADs. A colored dot displayed at the respective test zone indicates a positive result (presence of analytes). The absence of colored dots at the respective test zones indicates a negative result (absence of analytes) for that particular qualitative assay. \* (-) Negative; (+) Positive. Note: To avoid false-positive results in the reaction zones due to staining from conjugated nanomaterials, nanoparticles-labeled antibodies (conjugates) should not be dropped directly in the reaction zones for detection, but should be dropped in the region near to the reaction zones and then allowed to flow into their respective reaction zones for analysis. The size of the color dot looks different due to manual pipetting; however, the volume is the same (1  $\mu$ L). All colorimetric results are presented using a phone camera and desktop scanner. (For interpretation of the references to color in this figure legend, the reader is referred to the web version of this article.)

results. ACS patients with low risk can be treated as an unstable angina patient, and cardiac evaluation should be conducted to prevent heart damage and infarction after prolonged ischemia.

### 3.3. Calibration curve for quantitative assay

Quantitative colorimetric detection of the multiplex cardiac biomarkers GPBB, CK-MB, and cTnT, was performed by determining the reflectance of color intensity developed in the test zone(s) G, T, and M on the  $\mu$ PAD. The color intensity of GPBB, CK-MB, and cTnT on the fabricated  $\mu$ PAD was measured using the proposed reflectance detectors, phone camera, or scanner. As shown in Fig. 2, the calibration curve for reflectance detection of the color intensity of (a) GPBB, (b) CK-MB, and (c) cTnT on the  $\mu$ PAD was plotted. Then, the concentration of the unknown analytes was quantified by comparing the intensity in the test zones G, M, and T to the plotted calibration curve. The calibration curves for reflectance detection usually follow non-linear function of concentration (Teasdale et al., 1999). Non-linearity at a high concentration of the analytes occurs because of color saturation, whereas the limit of detection (LOD) of the developed  $\mu$ PADs for GPBB, CK-MB, and cTnT were  $0.5 \text{ ng mL}^{-1}$ ,  $0.5 \text{ ng mL}^{-1}$ , and  $0.05 \text{ ng mL}^{-1}$ , respectively, which was determined by the degree of visibility of the color dot in the test zones G, M, and T, respectively, on the fabricated  $\mu$ PAD. More importantly, the fabricated  $\mu$ PAD achieved a clinically significant visual LOD compared to the established POCT devices for the CK-MB assay (cutoff  $4\text{--}7 \text{ ng mL}^{-1}$ ) and cTnT assay (cutoff  $0.01\text{--}0.05 \text{ ng mL}^{-1}$ ). The cutoff values varied depending on the

manufacturer.

For quantification of cardiac biomarkers, the portable lateral flow strip reader is much more convenient and user-friendly compared to a bench-top analyzer in the central laboratory, which is still unaffordable for medical centers in developing countries. For example, a bench-top immunoassay analyzer costs approximately 50,000 £, whereas a portable reader costs almost 5,000 £, and easily available phone cameras and a scanner only cost  $\leq 100$  £. A desktop scanner was reported to provide reproducible result because the focus, image, and light conditions are constant (Carrilho et al., 2009b; Martinez et al., 2008, 2010). However, the quality of the images scanned from a desktop scanner is low and may have an impact when processed with image analyzer software programmed in a computer. In this study, the non-linearity at elevated quantities of analytes from the image captured by a phone camera was higher than that by a scanner, perhaps because the phone camera could capture good quality (resolution) images with better pixels than that by a desktop scanner. Cell phones are ubiquitous. If the resolution of the phone camera is sufficiently high, a portable phone camera can possibly function as an effective and accurate diagnostic tool in reflectance detection for semi-quantitative and quantitative data evaluation.

In addition, the binding affinity was determined using equilibrium dissociation constant (Kd) to evaluate the strength of biomolecular interactions. The smaller the Kd value, the greater was the binding affinity of the antibody with its target analyte. High affinity antibodies generally fall in the low nanomolar range ( $10^{-9}$  M) (An, 2011).  $K_{d1}$  was the dissociation constant calculated based on the images captured

**Table 2**

The signal intensity of each cardiac biomarker at each reaction zone, viz., G, (a) GPBB; M, (b) CK-MB; and T, (c) cTnT, on the fabricated  $\mu$ PADs with increasing concentration (left to right), representing the risk levels of heart condition as low, moderate, and high risk.

(a)	Concentration of GPBB (ng mL <sup>-1</sup> )	0	0.5	1	3	5	10	30	50	100
	(i) Phone camera									
	(ii) Scanner									
	Risk levels	Negative	Low			Moderate		High		
(b)	Concentration of CK-MB (ng mL <sup>-1</sup> )	0	0.5	1	3	5	10	30	50	100
	(i) Phone camera									
	(ii) Scanner									
	Risk levels	Negative	Low			Moderate		High		
(c)	Concentration of cTnT (ng mL <sup>-1</sup> )	0	0.05	0.1	1	5	10	50	100	200
	(i) Phone camera									
	(ii) Scanner									
	Risk levels	Negative	Low		Moderate			High		

via phone camera.  $K_{d2}$  was the dissociation constant calculated based on the images captured via a scanner.  $K_{d1}$  values for GPBB were  $K_{d1} = 2.22 \text{ ng mL}^{-1}$  ( $0.11 \times 10^{-9} \text{ M}$ ) and  $K_{d2} = 5.90 \text{ ng mL}^{-1}$  ( $0.31 \times 10^{-9} \text{ M}$ );  $K_{d1}$  values for CK-MB were  $K_{d1} = 6.98 \text{ ng mL}^{-1}$  ( $0.08 \times 10^{-9} \text{ M}$ ) and  $K_{d2} = 7.27 \text{ ng mL}^{-1}$  ( $0.08 \times 10^{-9} \text{ M}$ ); and  $K_{d1}$  values for cTnT were  $K_{d1} = 0.35 \text{ ng mL}^{-1}$  ( $0.01 \times 10^{-9} \text{ M}$ ) and  $K_{d2} = 1.71 \text{ ng mL}^{-1}$  ( $0.05 \times 10^{-9} \text{ M}$ ) (Fig. S10, Supplementary material). Comparison to other published works revealed that the antigen-binding affinities of these antibodies were high enough for use in sensitive immunoassays. Their  $K_{d}$  values were less than  $1 \times 10^{-9} \text{ M}$ , which were in low nanomolar range (Nakamura et al., 2010; Ramos-Vara and Miller, 2014). Pawula et al. (2016) reported a  $K_{d}$  value of  $3.28 \times 10^{-9} \text{ M}$  for cTnT, whereas Leickt et al. (2002) reported a  $K_{d}$  value ranging from  $10^{-8} - 10^{-10} \text{ M}$  for CK-MB based on peptide binding on a surface plasmon resonance (SPR) sensor. An aptamer-based fluorometric lateral flow assay produced a  $K_{d}$  value of  $14.74 \pm 1.86 \text{ nM}$  for CK-MB between the shortened aptamer (Zhang et al., 2018b).

### 3.4. Reproducibility, precision (intra- and inter-day), stability and cross-reactivity tests

In this study, other parameters for performance analysis of the fabricated  $\mu$ PAD comprised reproducibility, intra- and inter-day precision, stability and cross-reactivity tests performed using a phone camera and scanner. For the reproducibility test, relative standard deviation (RSD) obtained for GPBB, CK-MB, and cTnT were (i) 10.6% (G), 7.0% (M), 9.8% (T) and (ii) 12.2% (G), 10.2% (M), 8.5% (T), respectively, (Fig. S6) for the  $\mu$ PADs. The fabricated  $\mu$ PADs showed good reproducibility of the colorimetric results for multiple cardiac

biomarker measurements with  $\text{RSD} \pm 10\%$  for five replicates, indicating that the signals generated from the  $\mu$ PADs with the constant concentration of cardiac biomarkers were consistent.

Prior to ensuring that the fabricated  $\mu$ PAD meets the clinical specifications and can be used over a large concentration range, precision studies were performed at several concentration levels (low, medium, and high) across the working range on the same day and on three consecutive days with three replicates. Apple et al. (2005) described that the optimal precision for sensitive assay is considered at co-efficient of variation (CV) of  $\leq 10\%$ , but that  $> 10\%$  CV is also acceptable and does not cause false-positive results. However, only assays with  $\text{CV} > 20\%$  at the 99th percentile concentration are not recommended for use (Apple et al., 2005; Jaffe et al., 2010). For intra- and inter-day precision, the  $\mu$ PAD yielded results in the acceptable range of  $> 10\%$  to  $\leq 20\%$  for each cardiac biomarker, viz., GPBB, CK-MB, and cTnT, with concentrations of  $10 \text{ ng mL}^{-1}$ ,  $50 \text{ ng mL}^{-1}$ , and  $100 \text{ ng mL}^{-1}$ , respectively, (Fig. S7), which fulfilled the analytical criteria for clinical usage.

For the stability test, the fabricated  $\mu$ PAD surface was stable and retained (i) 91.2% (G), 85.5% (M), and 93.3% (T), and (ii) 86.2% (G), 78.1% (M), and 89.9% (T) of its detection ability after storage up to 28 days ( $N = 3$ ) (Fig. S8). The high stability of the fabricated  $\mu$ PAD can be ascribed to the high protein-binding affinity of the NC membrane by protein immobilization (Holstein et al., 2016). As result, the fabricated  $\mu$ PAD surface was stable, and the immobilized primary capture antibodies remained 70–90% active and were accessible to the target biomarkers (analytes) on the NC membrane over 28 days. In addition, the two-tailed  $t$ -test was performed to investigate the significance of the signal intensity differences observed during the study. Results at day 28 were compared to those obtained at day 1. No significant differences in

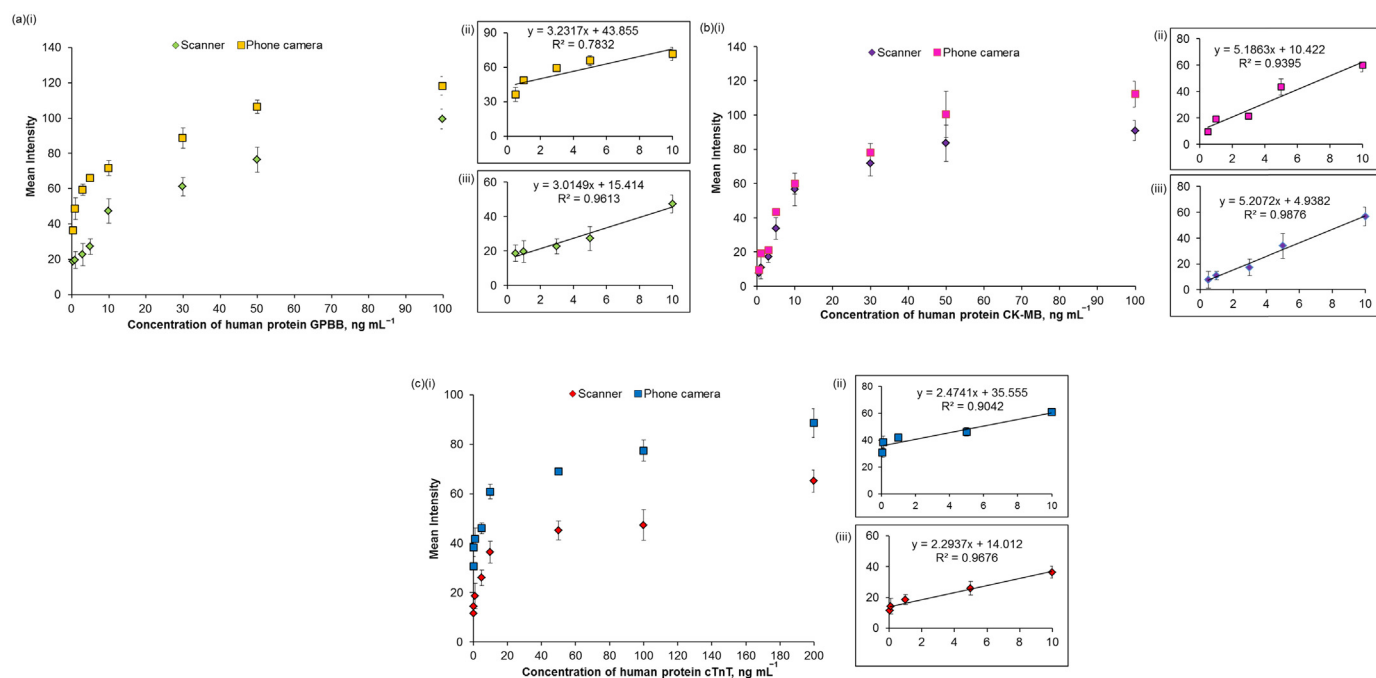


**Fig. 2.** Calibration curve for the quantitative detection of multiplex cardiac biomarkers using a (■) phone camera and (◆) desktop scanner. (a)(i) Signal intensity of test zone G measured versus concentrations of GPBB. Dynamic range obtained via (ii) phone camera and (iii) scanner. (b)(i) Signal intensity of test zone M measured versus concentrations of CK-MB. Dynamic range obtained via (ii) phone camera and (iii) scanner. (c)(i) Signal intensity of test zone T measured versus concentrations of cTnT. Dynamic range obtained via (ii) phone camera and (iii) scanner. Note: The mean of intensity for each data point was measured using the Image J software by selecting the area of the test zones G, M, and T for each assay in a digital image of the  $\mu$ PAD that was captured using a (■) phone camera and (◆) desktop scanner. Error bars represent the standard deviation for each data point (experiments were run in triplicates).

multiple cardiac biomarkers measurements were evident ( $p = 0.810$ ).

For the cross-reactivity test, the immobilized capture antibody on the fabricated  $\mu$ PAD did not cross-react with high levels of endogenous substances, including human serum albumin ( $100 \text{ mg mL}^{-1}$ ), uric acid ( $100 \mu\text{g mL}^{-1}$ ), and ascorbic acid ( $100 \mu\text{g mL}^{-1}$ ) in human serum containing cardiac biomarkers, since the results obtained for the spiked samples and un-spiked samples (with cardiac biomarkers only) were not significantly different (Fig. S9). These results indicated that the immobilized capture antibody at each reaction zone of the fabricated  $\mu$ PAD were highly selective for their respective cardiac biomarker (GPBB, CK-MB, and cTnT). An ANOVA test was performed to investigate the significance of the signal intensity differences observed between the three groups of un-spiked samples and cross-reactant spiked samples. No significant differences in the measurements of multiple cardiac biomarkers between un-spiked samples and spiked samples with each type of cross-reactant (human serum albumin, uric acid, and ascorbic acid) were evident ( $p = 0.976$ ,  $1.000$ , and  $0.999$ , respectively).

### 3.5. Real sample analysis and comparison of the methods

The fabricated  $\mu$ PAD was used to explore the practicability of detecting biomarker levels in clinical samples. The calibration curve was plotted for determination of CK-MB levels using actual human sera containing known amounts of CK-MB, which were obtained from University Malaya Medical Center. Both the calibration plots developed based on signals obtained from phone camera and scanner showed good linear regression with  $r^2 = 0.962$  ( $y = 3.1195x + 30.545$ ) and  $r^2 = 0.941$  ( $y = 2.3762x + 14.681$ ), respectively (Fig. 3a). On the other hand, points marked as 1, 2, and 3 were the three CK-MB concentrations determined for three unknown human sera obtained from University Malaya Medical Center. Using the calibration plot, the CK-MB levels in the three unknown human serum samples were calculated and the reliability and accuracy of obtained results were validated using the

signal measured through the Siemen Centaur XPT immunoassay system (a standard method) at the University Malaya Medical Center.

Analysis of method validation was performed using linear regression analysis and Bland–Altman plots between these three methods, i.e., I, II, and III for total 12 human serums samples. Linear regression analysis was conducted to study the relationships between two quantitative variables on the fabricated  $\mu$ PAD (II or III), and the findings were compared with the standard method (I). An excellent correlation was observed between I and II with  $r^2$  of 0.962 ( $y = 0.9759x + 0.114$ ) [Fig. 3b (i)], and an excellent correlation was also observed between I and III with  $r^2$  of 0.941 ( $y = 1x + 0.219$ ) [Fig. 3b (ii)]. The proposed methods II ( $r^2 = 0.962$ ) and III ( $r^2 = 0.941$ ) for CK-MB detection promise practical reliability as they exhibited a good fit with  $r^2$  of close to 1, with 96.2% and 94.1% variance of the observed values falling within the regression line. Bland–Altman plot difference shown in Fig. 3c was designed to describe the average bias (mean) relative to the reference method and the limits of agreement (95% of the differences). The resulting graph was a scatter plot, in which the difference of the two paired measurements was plotted against the mean of the two measurements. The mean difference should lie within 95% limit of agreement (mean bias  $\pm 1.96$  SD) (Giavarina, 2015). Based on the Bland–Altman plot, Fig. 3c (i) shows that the bias (difference between the means) was  $-0.060$  and the 95% limit of agreement was between  $-1.499$  and  $1.379$ . Fig. 3c (ii) shows that the bias (difference between the means) was  $-0.34\%$ , and 95% limit of agreement was between  $-2.357$  and  $1.668$ . All the differences were within the mean of  $-1.96$  SD (lower limit of agreement) and mean  $+1.96$  SD (upper limit of agreement). Moreover, this scatter plot also allowed us to investigate any possible relationship between the measurement error and the true value (Giavarina, 2015). The mean of difference equal to zero indicates that exactly the same results were obtained in measurements from the two methods. However, any measurement of variables always involves some degree of error. Compared to I, the mean bias of II ( $-0.060$ ) was closer to zero than that of III ( $-0.34$ ), indicating the good agreement

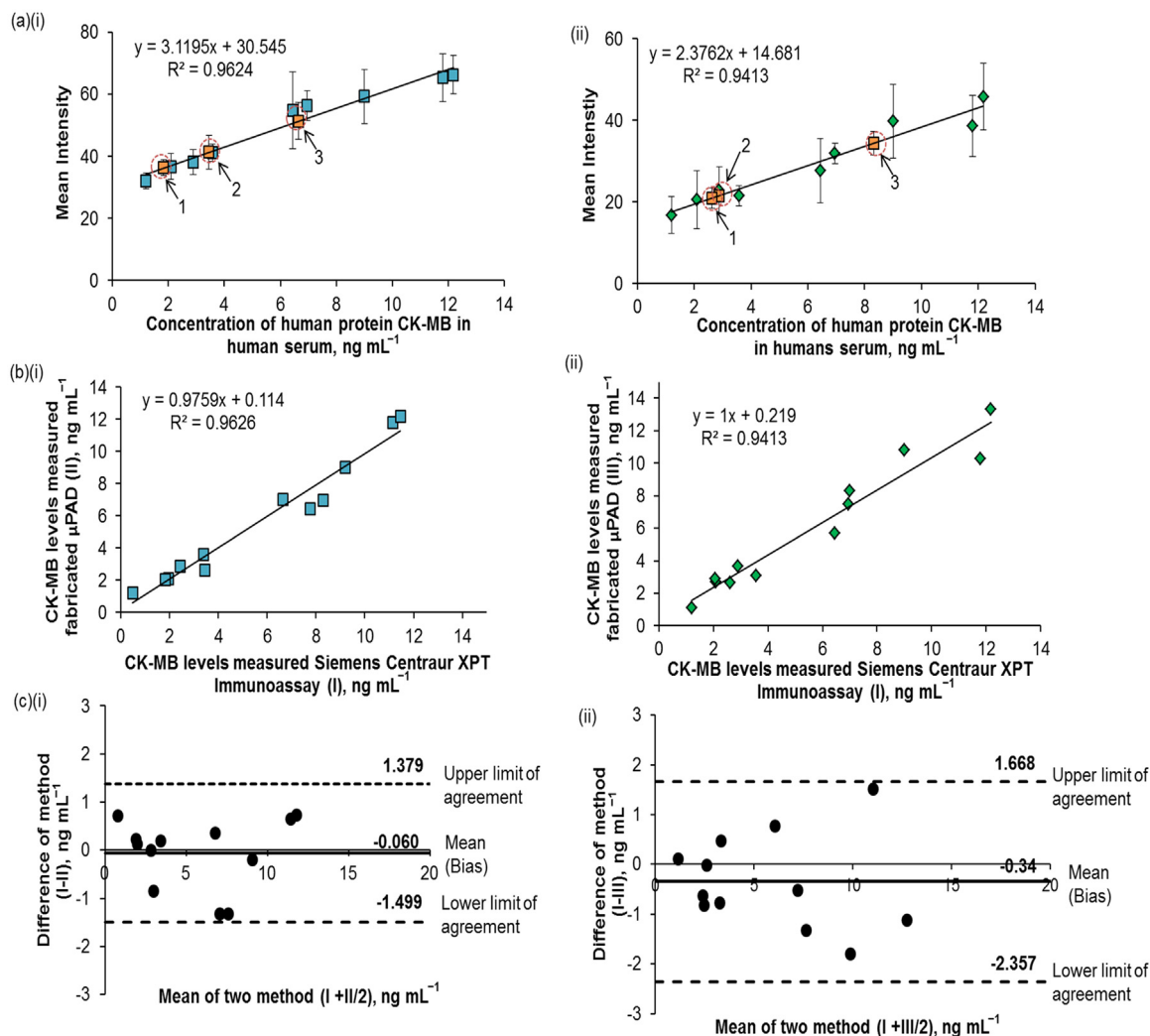


**Fig. 3.** (a) Calibration plots of CK-MB detection in actual human serum obtained from the University Malaya Medical Center. Color intensity was measured using (i) fabricated  $\mu$ PADs (phone camera) and (ii) fabricated  $\mu$ PADs (scanner). The concentrations of three unknown human serum samples containing CK-MB (obtained from the University Malaya Medical Center) were also determined and marked as 1, 2, and 3 based on the plotted calibration plot. *Note: Error bars represent the standard deviation for each data point (experiments were run in triplicates).* (b) Linear regression test between the Siemens Centaur XPT immunoassay system (I) and fabricated  $\mu$ PAD phone camera (II) and scanner (III) by measuring three replicates of 12 serum samples. (c) Bland–Altman plot of the 12 serum samples in which CK-MB concentration was measured using the reference and proposed methods. Solid line represents mean (bias), upper dashed line indicates the mean + 1.96 SD (upper limit of agreement), and lower dashed line indicates mean – 1.96 SD (lower limit of agreement). (For interpretation of the references to color in this figure legend, the reader is referred to the web version of this article).

between methods I and II, as they systematically produced equivalent results. Furthermore, II also showed narrower limits of agreement (between -1.499 and 1.379) than that by III (between -2.357 and 1.668), indicating that II is reasonably comparable with I, whereas III showed a wider limit range, reflecting less precision and ambiguous results.

In addition, paired sample *t*-test was performed to investigate the significance of the signal intensity differences observed in CK-MB levels of 12 human sera samples during the study. There was no significant difference between the levels determined by method I and the proposed  $\mu$ PAD using method II or III as the *p*-values were 0.352 and 0.151, respectively (*p* < 0.05 was considered significantly different).

The collective findings indicate that our fabricated  $\mu$ PAD showed an excellent concordance with the calibration and reference method in CK-MB assay. Moreover, the results revealed that a phone camera is nearly as effective as the reference method Siemens Centaur XPT immunoassay system for acquiring quantitative data. All types of phone cameras can be used but using a high pixel model of camera (not less than 13 megapixels) is recommended to capture high resolution images for

interpretation, similar to this study.

#### 4. Conclusions

An inexpensive and disposable  $\mu$ PAD was developed for simultaneous colorimetric determination of multiplex cardiac markers by using only an available phone camera and/or desktop scanner for quantification, which significantly decreased the analysis time (10 min) and reduced the cost for multiple marker measurement. A combination testing of the early marker GPBB with CK-MB and cTnT on the  $\mu$ PAD offers the best approach to include all symptoms of ACS for early diagnosis (ischemic myocardial injury) and prognosis of AMI to prompt diagnosis and save the individual from suffering a heart attack. The analytical performances of the fabricated  $\mu$ PAD yielded good results in this study. In addition, the clinical sample for CK-MB was analyzed using the fabricated  $\mu$ PAD to validate its capability in clinical practice. The result of comparison revealed that the measurements by the fabricated  $\mu$ PAD (detected using phone camera) are reproducible and highly correlated to the reference method (Siemens Centaur XPT

Immunoassay System). A phone camera appears to be a promising alternative technique compared to the expensive laboratory analyzer needed for quantification of biomarkers in developing countries or rural clinics. In this method, three different colored NPs (gold, silver, and gold urchin) were used as detecting indicators for a particular analyte, aiding the medical personnel to instantly distinguish the patient's condition. For future work, more effort is required to collect databases of colorimetric results and to program the results into a smart-based mobile phone that functions as a digital reader for health monitoring and disease diagnosis. The  $\mu$ PAD should prove valuable in diagnosis, providing better healthcare, reducing waiting time for result dissemination, and increasing the survival rate by rapid exclusion of MI.

## Acknowledgements

This work was financially supported by the University of Malaya postgraduate grant (PPP) (PG021–2015A), the Fundamental Research Grant Scheme (FRGS) from the Ministry of Higher Education of Malaysia (MOHE) (FP041–2016), and the Research University Grant (GPF057B-2018).

## Credit author statement

Wei Yin Lim carried out the experiments and wrote the manuscript. Sook Mei Khor and Boon Tong Goh supervised the project. Sook Mei Khor conceived the original idea, provided financial support, reviewed and edited the manuscript. Boon Tong Goh contributed in fabrication of microfluidic-paper based device, provided financial support and resources for the project and revised the manuscript. T. Malathi Thevarajah provided resources and contributed in the validation of human serum analysis in this project.

## Declaration of interest statement

This manuscript has not been published or presented elsewhere in part or in entirety, and is not under consideration by another journal. All the authors have approved the manuscript and agree with submission to your esteemed journal.

## Appendix A. Supporting information

Supplementary data associated with this article can be found in the online version at doi:10.1016/j.bios.2018.12.049.

## References

Al-Hadi, H.A., Fox, K.A., 2009. Sultan Qaboss Univ. Med. J. 9 (3), 231.  
 Amundson, B.E., Apple, F.S., 2015. Clin. Chem. Lab. Med. 53 (5), 665–676.  
 An, Z., 2011. John Wiley & Sons, United States.  
 Anderson, J.L., Adams, C.D., Antman, E.M., Bridges, C.R., Califf, R.M., Casey, D.E., Chavey, W.E., Fesmire, F.M., Hochman, J.S., Levin, T.N., 2007. J. Am. Coll. Cardiol. 50 (7), e1–e157.  
 Apple, F.S., Parvin, C.A., Buechler, K.F., Christenson, R.H., Wu, A.H., Jaffe, A.S., 2005. Clin. Chem. 51 (11), 2198–2200.  
 Arruebo, M., Valladares, M., Gonzalez-Fernandez, A., 2009. J. Nanomater.  
 Bertrand, M., Simoons, M., Fox, K., Wallentin, L., Hamm, C., McFadden, E., De Feyter, P., Specchia, G., Ruzyllo, W., 2000. Eur. Heart J. 21 (17), 1406–1432.  
 Bozkurt, S., Kaya, E.B., Okutucu, S., Aytemir, K., Coskun, F., Oto, A., 2011. Cardiol. J. 18

(5), 496–502.  
 Cai, Y., Kang, K., Li, Q., Wang, Y., He, X., 2018. Molecules 23 (5).  
 Carrilho, E., Martinez, A.W., Whitesides, G.M., 2009a. Anal. Chem. 81 (16), 7091–7095.  
 Carrilho, E., Phillips, S.T., Vella, S.J., Martinez, A.W., Whitesides, G.M., 2009b. Anal. Chem. 81 (15), 5990–5998.  
 Cho, J.H., Kim, M.H., Mok, R.S., Jeon, J.W., Lim, G.S., Chai, C.Y., Paek, S.H., 2014. J. Chromatogr. B 967, 139–146.  
 Choi, D.H., Lee, S.K., Oh, Y.K., Bae, B.W., Lee, S.D., Kim, S., Shin, Y.B., Kim, M.G., 2010. Biosens. Bioelectron. 25 (8), 1999–2002.  
 Cubranic, Z., Madzar, Z., Matijevec, S., Dvornik, S., Fistic, E., Tomulic, V., Kunisek, J., Laskarin, G., Kardum, I., Zaputovic, L., 2012. Biochem. Med. 22 (2), 225–236.  
 De Winter, R.J., Koster, R.W., Sturk, A., Sanders, G.T., 1995. Circulation 92 (12), 3401–3407.  
 Dincer, C., Bruch, R., Kling, A., Dittrich, P.S., Urban, G.A., 2017. Trends Biotechnol. 35 (8), 728–742.  
 Giavarina, D., 2015. Biochem. Med. 25 (2), 141–151.  
 Gupta, S., Singh, K.N., Bapat, V., Mishra, V., Agarwal, D.K., Gupta, P., 2008. Indian J. Clin. Biochem. 23 (1), 89–91.  
 Holstein, C.A., Chevalier, A., Bennett, S., Anderson, C.E., Keniston, K., Olsen, C., Li, B., Bales, B., Moore, D.R., Fu, E., Baker, D., Yager, P., 2016. Anal. Bioanal. Chem. 408 (5), 1335–1346.  
 Jaffe, A.S., Apple, F.S., Morrow, D.A., Lindahl, B., Katus, H.A., 2010. Clin. Chem. 56 (6), 941–943.  
 Kaski, J.C., Holt, D.W., 2013. Springer Science & Business Media, Germany.  
 Kim, T.K., Oh, S.W., Hong, S.C., Mok, Y.J., Choi, E.Y., 2014. J. Clin. Lab. Anal. 28 (6), 419–427.  
 Kontos, M.C., Diercks, D.B., Kirk, J.D., 2010. Mayo Clin. Proc. 85 (3), 284–299.  
 Lang, K., Börner, A., Figulla, H., 2000. J. Intern. Med. 247 (1), 119–123.  
 Lee, L.G., Nordman, E.S., Johnson, M.D., Oldham, M.F., 2013. Biosensors 3 (4), 360–373.  
 Leick, L., Grubb, A., Ohlson, S., 2002. Scand. J. Clin. Lab. Invest. 62 (6), 423–429.  
 Lopez-Ruiz, N., Curto, V.F., Erenas, M.M., Benito-Lopez, F., Diamond, D., Palma, A.J., Capitan-Vallvey, L.F., 2014. Anal. Chem. 86 (19), 9554–9562.  
 Mair, J., Artner-Dworzak, E., Lechleitner, P., Morass, B., Smidt, J., Wagner, I., Dienstl, F., Puschendorf, B., 1992. Br. Heart J. 68 (11), 462–468.  
 Martinez, A.W., Phillips, S.T., Carrilho, E., Thomas, S.W., Sindi, H., Whitesides, G.M., 2008. Anal. Chem. 80 (10), 3699–3707.  
 Martinez, A.W., Phillips, S.T., Whitesides, G.M., Carrilho, E., 2010. Anal. Chem. 82 (1), 3–10.  
 McDonnell, B., Hearty, S., Leonard, P., O'Kennedy, R., 2009. Clin. Biochem. 42 (7), 549–561.  
 Mythili, S., Malathi, N., 2015. Biomed. Rep. 3 (6), 743–748.  
 Nakamura, M., Ohta, H., Kume, N., Hayashida, K., Tanaka, M., Mitsuoka, H., Kaneshige, T., Misaki, S., Imagawa, K., Shimosako, Ki, 2010. J. Pharm. Biomed. Anal. 51 (1), 158–163.  
 Ohman, E.M., Armstrong, P.W., Christenson, R.H., Granger, C.B., Katus, H.A., Hamm, C.W., O'hanesian, M.A., Wagner, G.S., Kleiman, N.S., Harrell Jr, F.E., 1996. N. Engl. J. Med. 335 (18), 1333–1342.  
 Oncescu, V., Mancuso, M., Erickson, D., 2014. Lab Chip 14 (4), 759–763.  
 Oncescu, V., O'Dell, D., Erickson, D., 2013. Lab Chip 13 (16), 3232–3238.  
 Overbaugh, K.J., 2009. Am. J. Nurs. 109 (5), 42–52 (quiz 53).  
 Pawula, M., Altintas, Z., Tothill, I.E., 2016. Talanta 146, 823–830.  
 Quesada-Gonzalez, D., Merkoci, A., 2015. Biosens. Bioelectron. 73, 47–63.  
 Qureshi, A., Gurbuz, Y., Niazi, J.H., 2012. Sens. Actuators B 171, 62–76.  
 Ramos-Vara, J., Miller, M., 2014. Vet. Pathol. 51 (1), 42–87.  
 Rong-Hwa, S., Shiao-Shek, T., Der-Jiang, C., Yao-Wen, H., 2010. Food Chem. 118 (2), 462–466.  
 Ryu, Y., Jin, Z., Kang, M.S., Kim, H.-S., 2011. BioChip J. 5 (3), 193–198.  
 Sechi, D., Greer, B., Johnson, J., Hashemi, N., 2013. Anal. Chem. 85 (22), 10733–10737.  
 Shen, L., Hagen, J.A., Papautsky, I., 2012. Lab Chip 12 (21), 4240–4243.  
 Teasdale, P.R., Hayward, S., Davison, W., 1999. Anal. Chem. 71 (11), 2186–2191.  
 Van de Werf, F., Ardissino, D., Betriu, A., Cokkinos, D.V., Falk, E., Fox, K.A., Julian, D., Lengyel, M., Neumann, F.J., Ruzyllo, W., Thygesen, C., Underwood, S.R., Vahanian, A., Verheugt, F.W., Wijns, W., Task Force on the Management of Acute Myocardial Infarction of the European Society of, C., 2003. Eur. Heart J. 24 (1), 28–66.  
 Veigas, B., Jacob, J.M., Costa, M.N., Santos, D.S., Viveiros, M., Inacio, J., Martins, R., Barquinha, P., Fortunato, E., Baptista, P.V., 2012. Lab Chip 12 (22), 4802–4808.  
 Yen, C.-W., de Puig, H., Tam, J.O., Gómez-Márquez, J., Bosch, I., Hamad-Schifferli, K., Gehrke, L., 2015. Lab Chip 15 (7), 1638–1641.  
 Zhang, D., Huang, L., Liu, B., Ni, H.B., Sun, L.D., Su, E.B., Chen, H.Y., Gu, Z.Z., Zhao, X.W., 2018a. Biosens. Bioelectron. 106, 204–211.  
 Zhang, J., Lv, X., Feng, W., Li, X., Li, K., Deng, Y., 2018b. Microchim. Acta 185 (8), 364.